

Interactions of Impaired Glucose Transport and Phosphorylation in Skeletal Muscle Insulin Resistance

A Dose-Response Assessment Using Positron Emission Tomography

Katherine V. Williams,¹ Julie C. Price,² and David E. Kelley^{1,3}

It has been postulated that glucose transport is the principal site of skeletal muscle insulin resistance in obesity and type 2 diabetes, though a distribution of control between glucose transport and phosphorylation has also been proposed. The current study examined whether the respective contributions of transport and phosphorylation to insulin resistance are modulated across a dose range of insulin stimulation. Rate constants for transport and phosphorylation in skeletal muscle were estimated using dynamic positron emission tomography (PET) imaging of 2-deoxy-2-[¹⁸F]fluoro-D-glucose ([¹⁸F]FDG) during insulin infusions at three rates (0, 40, and 120 mU/m² per min) in lean glucose-tolerant, obese glucose-tolerant, and obese type 2 diabetic subjects. Parallel studies of arteriovenous fractional extraction across the leg of [¹⁸F]FDG and [2-³H] glucose were performed to measure the "lumped constant" (LC) (i.e., the analog effect) for [¹⁸F]FDG to determine whether this value is affected by insulin dose or insulin resistance. The value of the LC was similar across insulin doses and groups. Leg glucose uptake (LGU) also provided a measure of skeletal muscle glucose metabolism independent of PET. [¹⁸F]FDG uptake determined by PET imaging strongly correlated with LGU across groups and across insulin doses ($r = 0.81$, $P < 0.001$). Likewise, LGU correlated with PET parameters of glucose transport ($r = 0.67$, $P < 0.001$) and glucose phosphorylation ($r = 0.86$, $P < 0.001$). Glucose transport increased in response to insulin in the lean and obese groups ($P < 0.05$), but did not increase significantly in the type 2 diabetic group. A dose-responsive pattern of stimulation of glucose phosphorylation was observed in all groups of subjects ($P < 0.05$); however, glucose phosphorylation was lower in both the obese and type 2 diabetic groups compared with the lean group at the moderate insulin dose ($P < 0.05$). These

findings indicate an important interaction between transport and phosphorylation in the insulin resistance of obesity and type 2 diabetes. *Diabetes* 50:2069–2079, 2001

During the past several years, several methodologies for in vivo studies in humans of insulin regulation of glucose transport and phosphorylation in skeletal muscle have been developed. These methods include a triple tracer forearm method (1,2), magnetic resonance spectroscopy (MRS) imaging of glucose-6-phosphate (G-6-P) (3,4) and, more recently, free glucose (5), and dynamic positron emission tomography (PET) imaging using the glucose analog 2-deoxy-2-[¹⁸F]fluoro-D-glucose ([¹⁸F]FDG) (6,7). A consistent finding from these three methods has been to confirm the importance of glucose transport (1,2,5–7), and this finding is consistent with data from animal studies (8). However, in vivo human studies also indicate that glucose phosphorylation may mediate control of insulin-stimulated glucose metabolism in skeletal muscle and contribute to insulin resistance (1,2,6,7). Formation of G-6-P, the reaction catalyzed by hexokinase, traps glucose within myocytes, preventing outward transport and sustaining a gradient for free glucose flux across sarcolemma (9). In addition, utilization of ATP in formation of G-6-P has a major role in ATP-ADP exchange in mitochondria and thus in the regulation of oxidative phosphorylation (9).

In skeletal muscle in lean healthy individuals, insulin enhances the efficiency of glucose phosphorylation (1,6). Dose-responsive studies in lean individuals suggest an important contribution of glucose phosphorylation to the control of glucose utilization (7). The distribution of control between glucose transport and phosphorylation suggests that phosphorylation has an important regulatory contribution during moderate insulin stimulation, whereas transport may limit utilization at marked insulin stimulation (7). This pattern of normal physiology raises the question of the respective contributions of glucose transport and phosphorylation to insulin resistance. In investigations in patients with type 2 diabetes using either PET imaging of [¹⁸F]FDG (6) or the forearm triple tracer method (2), insulin resistance in skeletal muscle appears to involve impediments of both glucose transport and glucose phosphorylation. Although these findings are consistent

From the ¹Department of Medicine and ²Department of Radiology, University of Pittsburgh, Pittsburgh, Pennsylvania; and ³Medical Research Service, Pittsburgh Veterans Affairs Medical Center, Pittsburgh, Pennsylvania.

Address correspondence and reprint requests to David E. Kelley, MD, Professor of Medicine, University of Pittsburgh School of Medicine, Division of Endocrinology and Metabolism, 810N, 3459 Fifth Ave., Pittsburgh, PA 15261. E-mail: kelley@msx.dept-med.pitt.edu.

Received for publication 23 February 2000 and accepted in revised form 13 June 2001.

2D, two-dimensional; 3D, three-dimensional; [2-³H]G, [2-³H]glucose; [¹⁸F]FDG, 2-deoxy-2-[¹⁸F]fluoro-D-glucose; CT, computed tomography; DV, distribution volume; E, fractional extraction; G-6-P, glucose-6-phosphate; HPLC, high-performance liquid chromatography; LC, lumped constant; LGU, leg glucose uptake; MRS, magnetic resonance spectroscopy; PET, positron emission tomography; PF, phosphorylation fraction; ROI, region of interest.

with a distribution of control between transport and phosphorylation in mediating insulin resistance, it remains unknown whether this is a dynamic or a fixed relationship in the pathophysiology of insulin resistance. A recent study using MRS to estimate intracellular free glucose concentration in skeletal muscle found no substantial accumulation in type 2 diabetes during marked insulin concentrations (5) and accordingly concluded that glucose transport is the predominant site of insulin resistance in type 2 diabetes. However, it remains unclear whether this interpretation is fully applicable across a range of insulin concentration. For example, in the study by Cline et al. (5), skeletal muscle in type 2 diabetic patients versus lean control subjects had a lesser increment in G-6-P during moderate insulin concentrations, yet showed somewhat higher muscle free glucose concentrations (though not significantly different). At marked insulin stimulation, the deficit of G-6-P was partially corrected, whereas free glucose was lower than in control subjects. Thus, although these findings are consistent with glucose transport being rate-limiting at marked insulin concentration, the question persists of whether a redistribution of control might also be effected by insulin even in the setting of insulin resistance.

The primary purpose of the current study was to examine dose-response effects of insulin (i.e., basal, moderate, and high steady-state concentrations) on the regulation of glucose transport and glucose phosphorylation within skeletal muscle in obesity and type 2 diabetes, as compared with lean healthy volunteers. A second purpose of our study was to assess the analog effect of [¹⁸F]FDG relative to glucose, an effect generally termed the lumped constant (LC). Our laboratory (10) and others (11) recently reported a value of ~1.2 for skeletal muscle in lean healthy volunteers. The LC has not been evaluated with respect to insulin resistance, and this is of importance in comparing insulin-sensitive and insulin-resistant subjects. To perform studies of the LC and to compare data from PET imaging with an independently derived measure of insulin-stimulated glucose metabolism by skeletal muscle, arteriovenous limb balance studies across the leg were carried out during steady-state metabolic conditions, simultaneously with PET imaging.

RESEARCH DESIGN AND METHODS

Subjects. A total of 42 research volunteers participated in this study. They were categorized into three groups (lean glucose-tolerant subjects, *n* = 14; obese glucose-tolerant subjects, *n* = 15; and obese subjects with type 2 diabetes, *n* = 13). Subjects were recruited by advertisement. Before participating in this study, each volunteer had a medical examination. Participants were of stable weight, in good general health, and with normal values for hematological, renal, thyroid, and hepatic function. The University of Pittsburgh Institutional Review Board approved the investigation, and all volunteers gave written informed consent.

Characteristics of study subjects are shown in Table 1. Groups did not differ in sex distribution. Overall, the three groups differed in age (lean 37 ± 1 years, obese 42 ± 2 years, and obese with type 2 diabetes 50 ± 2 years, mean ± SE, *P* < 0.001). Obese subjects with and without type 2 diabetes had similar BMIs. Fasting plasma glucose and HbA_{1c} levels were higher in subjects with type 2 diabetes (*P* < 0.001), and obese subjects and obese type 2 diabetic subjects had fasting hyperinsulinemia as compared with lean volunteers. Subjects with type 2 diabetes were under good glycemic control at entry to the study and were treated with diet alone (*n* = 2) or sulfonylureas (*n* = 11), and all diabetes medications were withdrawn at least 2 weeks before the studies. The mean known duration of type 2 diabetes was 4.5 ± 1.0 years. Four obese subjects reported a family history of type 2 diabetes. The majority of subjects were normotensive. Two obese subjects had diastolic blood pressure readings

TABLE 1
Baseline characteristics of study subjects

| | Lean subjects | Obese subjects | Type 2 diabetic patients |
|---------------------------------|---------------|----------------|--------------------------|
| Sex (<i>n</i>) | 12M/2F | 11M/4F | 8M/5F |
| Age (years) | 37 ± 1* | 42 ± 2* | 50 ± 2* |
| BMI (kg/m ²) | 24.9 ± 0.4* | 32.4 ± 0.7* | 32.3 ± 0.8* |
| Fasting plasma glucose (mmol/l) | 4.5 ± 0.1* | 5.2 ± 0.1* | 9.5 ± 3.7* |
| HbA _{1c} (%) | 5.0 ± 0.1* | 5.3 ± 0.1* | 7.2 ± 0.3* |
| Fasting insulin (pmol/l) | 30 ± 5* | 84 ± 18* | 96 ± 12* |

Data are means ± SE, unless otherwise indicated. **P* < 0.001 for overall three-group comparisons.

between 90 and 100 mmHg and three subjects with type 2 diabetes were receiving antihypertensive therapy.

Study design. The study protocol is shown in Fig. 1. All subjects were randomly assigned to receive euglycemic insulin infusion at rates of 0, 40, or 120 mU/m² per min. Within insulin dose assignment, the subjects did not differ by baseline characteristics. Subjects were admitted to the University of Pittsburgh General Clinical Research Center on the evening before studies in order to standardize activity and the length of fast before studies. Subjects were instructed to ingest a diet containing at least 200 g carbohydrate for at least 3 days before admission and to refrain from exercise on the day preceding a study. On the evening of admission, subjects received a dinner of standardized composition (7 kcal/kg; 50% carbohydrate, 30% fat, and 20% protein), then fasted overnight until completion of the study.

Euglycemic-hyperinsulinemic clamp. On the morning of the study, an intravenous catheter was placed in an antecubital vein for infusion of insulin and glucose and for later injection of [¹⁸F]FDG and [2-³H]glucose ([2-³H]G) (high-performance liquid chromatography [HPLC] purified, New England Nuclear, Boston, MA). Catheters were placed in a radial artery and a femoral vein for blood sampling, which included the determination of the arterial concentrations of [¹⁸F]FDG for use as an input function in PET modeling, and for leg-balance studies. After basal measurements of arterial insulin and arterial and femoral venous glucose, an insulin infusion (or saline for basal dose of insulin) was initiated and continued for 270 min. During insulin infusion, arterial glucose was measured at 5 per min intervals, using a YSI Glucose Analyzer (Yellow Springs Instruments, Yellow Springs, OH). An adjustable infusion of 20% dextrose maintained euglycemia for 3 h before injection of [¹⁸F]FDG, so that steady-state metabolic conditions were attained.

Measurement of [¹⁸F]FDG uptake with PET. Subjects were positioned in the PET scanner after 150 min of insulin infusion so that the mid thigh corresponded to the midpoint axial field of view to obtain a transmission scan (Fig. 1). The transmission scan was performed using rotating rods of ⁶⁸Ge/⁶⁸Ga to correct the emission data for photon attenuation. This was followed by an intravenous injection of 4 mCi of [¹⁸F]FDG, synthesized using a modification of the method of Hamacher et al. (12) and [2-³H]G. A 90 per min dynamic PET scan was simultaneously initiated (19 frames: 4 × 30 s, 4 × 2 min, 6 × 5 min, and 5 × 10 min). Dynamic arterial sampling of [¹⁸F]FDG was also performed as described below. The PET scans were acquired in two-dimensional (2D) and three-dimensional (3D) imaging modes using a Siemens CTI 951 R/31 (*n* = 15) scanner, an ECAT ART scanner (*n* = 27). The imaging characteristics of the two scanners were comparable. The Siemens 951R/31 scanner acquired 31 imaging planes simultaneously (2D, in-plane resolution 6.0 mm FWHM [ramp

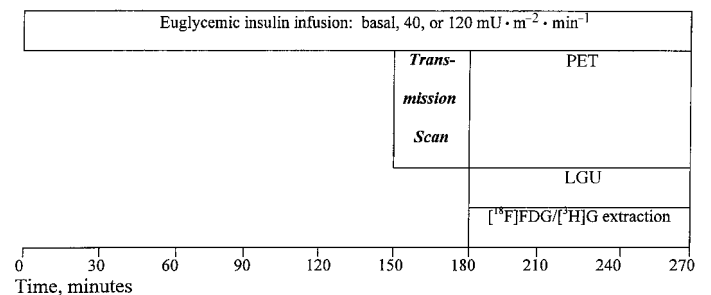


FIG. 1. Study protocol. Bolus injections of [¹⁸F]FDG and [³H]G were administered at 180 min. Arterial sampling was performed as described in the text.

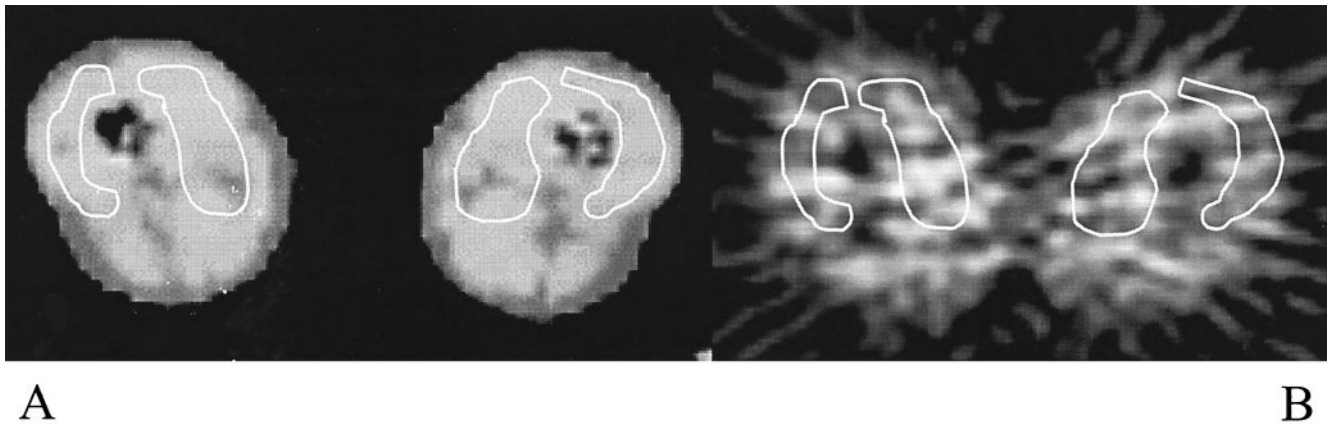


FIG. 2. ROIs were identified on the medial and lateral thigh muscles on the coregistered CT-transmission scan (A) and then applied to dynamic PET images (B).

filter], axial slice width: 3.4 mm), whereas 47 imaging planes were acquired using the ECAT ART scanner (3D, in-plane resolution 6.0 mm FWHM [ramp filter], axial slice width 3.4 mm). The scatter fraction was low for the 2D Siemens CTI 951 (13%) (13) and no scatter correction was performed following conventional methods. The 3D ART had a scatter fraction that was ~37% (14), and these emission data were corrected for scattered photons using a model-based correction method (15,16). A total of seven subjects (one obese and one with type 2 diabetes at the 40-unit dose and one lean, two obese, and two with type 2 diabetes at the 120-unit dose) had their studies limited to 60 min due to discomfort while lying on the scanning table.

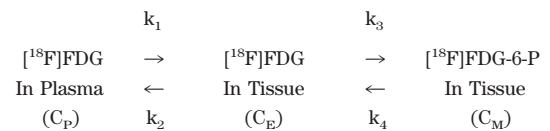
Defining regions of interest in skeletal muscle. To more clearly define skeletal muscle on PET images, three cross-sectional computed tomography (CT) scans of 1-cm thickness were obtained at upper, middle, and lower boundaries of the region of midthigh to be scanned during PET imaging. These CT images were coregistered with the matching PET transmission images as previously described (6). Regions of interest (ROIs) were drawn in medial and lateral thigh muscle using Imagetool (CTI PET Systems) software (Fig. 2A) and saved as template files for application to the PET images (Fig. 2B). The ROIs were applied across multiple planes of the dynamic PET scans after correction of the PET data for radioactive decay. The tissue time activity data within the ROIs were converted to units of radioactivity concentration ($\mu\text{Ci}/\text{ml}$) using an empirical phantom-based calibration factor ($\mu\text{Ci}/\text{ml}/\text{PET}$ counts per pixel).

Leg-balance studies. Arteriovenous balance studies of glucose, [^{18}F]FDG, and [$2\text{-}^3\text{H}$]G were performed at the University of Pittsburgh PET Center concurrent with PET scanning (Fig. 1), for the purpose of obtaining a measure of glucose uptake by leg tissue, for comparison with PET imaging data, and to assess the LC as described below. Blood flow to the leg was measured using venous occlusion strain-gauge plethysmography. During steady-state conditions, the rate of glucose uptake across the leg was calculated as the product of arteriovenous differences for glucose and blood flow according to the Fick principle. The mean of five determinations of blood flow and the mean of eight determinations of arteriovenous differences for glucose were used in the calculation. The arteriovenous extraction of glucose was determined under steady-state conditions during the last 90 min of the clamp study.

To determine the LC for [^{18}F]FDG, the fractional extractions of [^{18}F]FDG and [$2\text{-}^3\text{H}$]G across the leg were measured. Injections of 4 mCi of [^{18}F]FDG (described above) and 20 μCi of [$2\text{-}^3\text{H}$]G (HPLC purified, New England Nuclear), dissolved in 5 ml of normal saline, were administered via an antecubital venous catheter at the start of the PET study. Sampling of arterial and femoral venous blood for plasma [^{18}F]FDG and [$2\text{-}^3\text{H}$]G radioactivity were obtained at 6-s intervals for 2 min, 20-s intervals for 1 min, 30-s intervals for 1 min, and at 5, 7, 10, 15, 20, and 30 min, then every 15 min until 90 min postinjection of [^{18}F]FDG and [$2\text{-}^3\text{H}$]G. Exact timing of each sample was recorded. Blood was centrifuged and radioactivity in 0.2 ml of plasma was counted using a Packard Canbarra well counter. For determination of [^3H]G, these plasma samples were stored, frozen at -80°C , then later deproteinized, evaporated to dryness to remove tritiated water, reconstituted (scintillation liquid), and counted with liquid scintillation, as previously described (17).

Calculations. A three-compartment model was used to analyze the [^{18}F]FDG kinetics of the PET data (18–20) as previously described (7). Compartmental modeling, using the dynamically acquired PET data with the arterial plasma time course of [^{18}F]FDG activity (C_p) as a model input function, used a nonlinear least-squares method to iteratively derive values for the individual rate constants: k_1 (ml/min/ml), k_2 (min^{-1}), and k_3 (min^{-1}). The rate constants

represent inward transport (k_1), outward transport (k_2), and phosphorylation (k_3) of [^{18}F]FDG as shown below:



Dephosphorylation of [^{18}F]FDG-6-P, represented by the parameter k_4 (min^{-1}), was assumed to be negligible during these emission studies, in accord with prior data (21) and after preliminary estimates of this parameter revealed extremely small values ($<0.01 \text{ min}^{-1}$) in the current study.

Using the individual kinetic parameters, we calculated three additional parameters. The first is overall uptake rate of [^{18}F]FDG [$K = (k_1 \times k_3)/(k_2 + k_3)$, ml/min/ml]. The second, that of the ratio k_1/k_2 , (ml/ml), corresponds to the distribution volume of free (nonphosphorylated) [^{18}F]FDG (DV_{CE}) and reflects glucose transport. The inward transport rate constant, k_1 , reflects movement of tracer from plasma to a tissue compartment that includes both intracellular and interstitial space. Conceptually, the k_2 parameter represents movement of free [^{18}F]FDG from the “tissue” compartment back into plasma. However, it is conceivable that, anatomically, the “tissue” compartment for free [^{18}F]FDG could represent both the interstitial space and the intracellular space. Thus, k_2 might reflect [^{18}F]FDG that is returning to plasma from I the interstitial space, because it has not been transported into the myocyte and/or Z the myocyte, because it has been transported into the myocyte but not phosphorylated. Because the amount of free glucose in the intracellular space is regarded as very small with respect to interstitial space, an elevated value of k_2 may largely reflect free [^{18}F]FDG that has entered interstitial space from plasma but has not entered intracellular space. Thus, defects in glucose transport may be reflected both as reduced k_1 and increased k_2 . The phosphorylation fraction (PF) of [^{18}F]FDG [$\text{PF} = k_3/(k_2 + k_3)$] is a fraction with a potential range of 0 to 1, reflecting the disposition for nonphosphorylated [^{18}F]FDG within the tissue compartment to be phosphorylated (as $k_3 > k_2$) or to egress to the plasma compartment (as $k_2 > k_3$). It has been interpreted as an index of the extent to which glucose phosphorylation serves as the rate-limiting step of glucose metabolism relative to glucose transport (22).

To assess the analog effect of [^{18}F]FDG, we compared the extraction of this analog with that of nonanalog glucose represented by [$2\text{-}^3\text{H}$]G. Because [^{18}F]FDG is conventionally given as a bolus, the LC was determined based on a bolus injection of [^{18}F]FDG. To relate the extraction of a bolus injection of [^{18}F]FDG to a bolus of a nonanalog of glucose, [$2\text{-}^3\text{H}$]G was given simultaneously. The LC was calculated as the ratio between the fractional extraction of [^{18}F]FDG ($E_{[^{18}\text{F}]FDG}$) and that of [$2\text{-}^3\text{H}$]G ($E_{[2\text{-}^3\text{H}]G}$). Representative bolus curves of [^{18}F]FDG and [$2\text{-}^3\text{H}$]G are shown in Fig. 3. The non-steady-state fractional extractions (E) of [^{18}F]FDG and [$2\text{-}^3\text{H}$]G were determined based on the respective arterial (C_A) and femoral venous (C_V) plasma radioactivity concentration differences over the study period (23). The fractional extractions (E) were calculated over the study duration (T) such that:

$$E_{[^{18}\text{F}]FDG \text{ or } [2\text{-}^3\text{H}]G} = \frac{\sum_{i=1}^T (C_A - C_V)}{\sum_{i=1}^T C_A}$$

Because the arterial venous differences in extraction approximated zero by 60 min after bolus injection, the data were not extrapolated to infinity but were

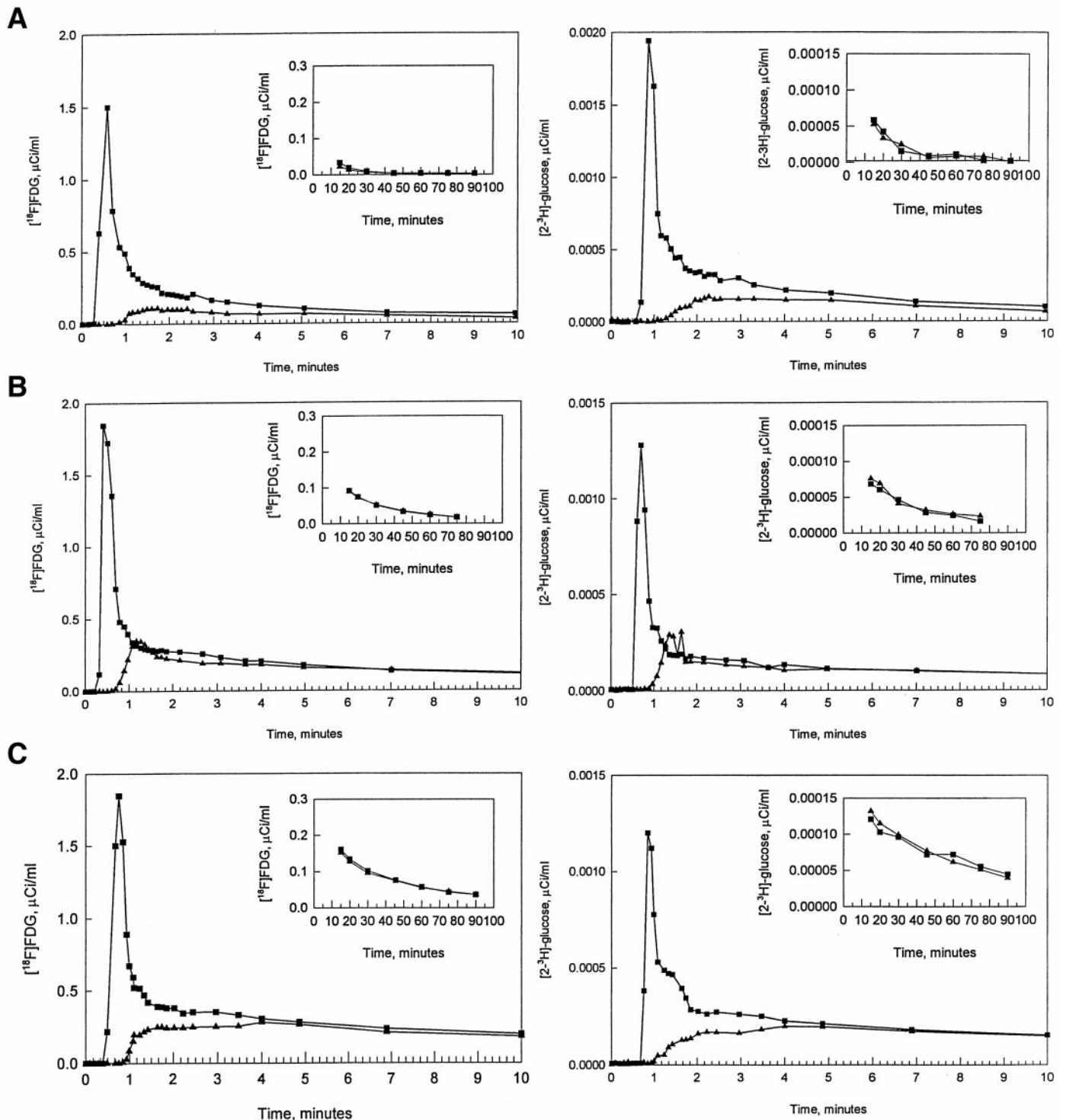


FIG. 3. Representative arterial and femoral venous plasma time-activity curves for $[^{18}\text{F}]\text{FDG}$ and $[^3\text{H}]\text{G}$ at insulin infusion of $40 \text{ mU}/\text{min} \cdot \text{m}^{-2}$ in lean (A), obese (B), and type 2 diabetic (C) subjects. ■, Arterial data; ▲, venous data. Data from later time points are shown in the inset graphs.

measured over a 90 per min period. Comparable values for the LC were obtained regardless of whether the data were analyzed over 60 or 90 min.

Statistics. Data are expressed as means \pm SE. Analysis of variance, with use of nonparametric analyses where appropriate, was used to examine the effects of insulin dose on the various metabolic parameters (e.g., leg glucose uptake [LGU]). Correlations and linear regression were used to examine associations between variables. A *P* value of <0.05 was considered significant.

RESULTS

Arteriovenous insulin-stimulated glucose uptake across the leg. Steady-state rates of LGU in lean, obese, and obese type 2 diabetic volunteers at basal, moderate, and high levels of insulin stimulation are shown in Table 2. Euglycemia was maintained during insulin infusions, ex-

TABLE 2
Insulin-stimulated glucose metabolism obtained by leg balance methods

| Insulin dose (mU/m ² per min) | Subjects (n) | Arterial glucose (mmol/l) | Plasma insulin (pmol/l) | Glucose infusion rate (mg/kg per min) | Arteriovenous glucose difference (mmol/l) | Blood flow (ml/min/100 ml leg tissue) | LGU (mg/min/100 ml leg tissue) | Fractional extraction of glucose (%) |
|--|--------------|---------------------------|-------------------------|---------------------------------------|---|---------------------------------------|--------------------------------|--------------------------------------|
| Basal (0) | | | | | | | | |
| Lean | 4 | 4.9 ± 0.1 | 53 ± 12 | 0.0 ± 0.0 | 0.1 ± 0.0 | 2.1 ± 0.4 | 0.04 ± 0.01 | 2.3 ± 0.4 |
| Obese | 4 | 5.5 ± 0.2 | 90 ± 14 | 0.0 ± 0.0 | 0.1 ± 0.0 | 2.4 ± 0.5 | 0.04 ± 0.01 | 1.9 ± 0.5 |
| Type 2 diabetic | 4 | 10.4 ± 2.6 | 92 ± 27 | 0.0 ± 0.0 | 0.2 ± 0.0 | 1.9 ± 0.3 | 0.05 ± 0.004 | 1.7 ± 0.3 |
| Moderate (40) | | | | | | | | |
| Lean | 6 | 5.3 ± 0.3 | 448 ± 11* | 8.4 ± 0.8* | 1.6 ± 0.3* | 2.7 ± 0.2 | 0.87 ± 0.28* | 30.9 ± 6.2* |
| Obese | 4 | 5.2 ± 0.1 | 596 ± 49* | 2.9 ± 0.3* | 0.5 ± 0.1* | 2.6 ± 0.6 | 0.24 ± 0.06* | 10.3 ± 1.2* |
| Type 2 diabetic | 4 | 5.5 ± 0.1 | 587 ± 23* | 1.9 ± 0.4* | 0.4 ± 0.0* | 2.3 ± 0.4 | 0.18 ± 0.05* | 7.9 ± 0.9* |
| High (120) | | | | | | | | |
| Lean | 4 | 5.1 ± 0.1 | 1,270 ± 64*† | 8.3 ± 0.4† | 2.2 ± 0.1† | 2.9 ± 0.3 | 1.13 ± 0.14† | 42.1 ± 2.2† |
| Obese | 7 | 5.1 ± 0.1 | 1,979 ± 154*† | 7.7 ± 0.9† | 1.9 ± 0.2† | 3.9 ± 0.6 | 1.30 ± 0.24† | 36.9 ± 4.2† |
| Type 2 diabetic | 5 | 5.3 ± 0.1 | 2,097 ± 356*† | 4.8 ± 1.2† | 1.4 ± 0.4† | 3.6 ± 0.7 | 0.83 ± 0.16† | 27.6 ± 7.3† |

Data are means ± SE, unless otherwise indicated. * $P < 0.05$, analysis of variance between groups (lean, obese, type 2 diabetic) within insulin dose; † $P < 0.05$, analysis of variance for significant change between insulin doses within group (lean, obese, type 2 diabetic).

cept that hyperglycemia (10.4 ± 2.6 mmol/l) persisted in subjects with type 2 diabetes who received a basal (zero rate) insulin infusion. Plasma insulin levels attained during the moderate and high rates of insulin infusion were similar in obese and diabetic subjects and were higher than in lean subjects ($P < 0.05$). The rate of steady-state systemic glucose infusion needed to maintain euglycemia (data not shown) differed by insulin dose ($P < 0.05$) and correlated with respective values for LGU ($r = 0.76$, $P < 0.001$).

Rates of glucose uptake across the leg increased in a dose-responsive manner across the three rates of insulin infusion (Table 2). Basal rates of LGU and fractional extraction of glucose were similar in all groups, but at the moderate rate of insulin infusion, LGU and fractional extraction of glucose were three- to fourfold greater in lean volunteers than in obese and type 2 diabetic subjects. At the high rate of insulin infusion, group differences were less evident, as rates of LGU and fractional extraction of glucose in obese and type 2 diabetic volunteers did not differ significantly from lean volunteers.

Rate constants for glucose transport and phosphorylation. Table 3 shows the overall rate of [¹⁸F]FDG clearance

(K) and the rate constants for inward transport (k_1), outward transport (k_2), and glucose phosphorylation (k_3). **Basal.** During basal conditions, the overall clearance of [¹⁸F]FDG by thigh muscle did not differ significantly in comparing obese and type 2 diabetic volunteers with lean subjects, nor were there significant group differences for the individual rate constants.

Moderate insulin infusion. In lean volunteers, the moderate rate of insulin infusion stimulated approximately an eight- to tenfold increase in the overall clearance of FDG compared with basal values, reaching a significantly higher mean value than in obese or type 2 diabetic volunteers (Table 3). In lean volunteers, values for k_3 increased approximately fivefold above basal during moderate insulin, whereas values for k_2 decreased. There was a significant group difference in values for k_2 , with higher values in the obese and type 2 diabetic subjects. No significant changes in any of the three rate constants were observed in obese or type 2 diabetic compared with respective basal values. The values for the DV_{CE} of FDG ($k_1:k_2$ ratio) and the PF [$k_3/(k_2 + k_3)$] were each significantly greater in lean compared with obese or type 2 diabetic subjects (Figs. 4 and 5). The values for DV_{CE} and PF were approximately

TABLE 3
Rate constants from three-compartment modeling of dynamic PET of [¹⁸F]FDG metabolism in skeletal muscle

| Insulin dose (mU/m ² per min) | K × 10 ⁻³ (mg/ml per min) | k_1 (ml/min per ml) | k_2 (min ⁻¹) | k_3 (min ⁻¹) |
|--|--------------------------------------|-----------------------|----------------------------|----------------------------|
| Basal (0) | | | | |
| Lean | 2.75 ± 0.86 | 0.028 ± 0.012 | 0.259 ± 0.058 | 0.030 ± 0.007 |
| Obese | 0.80 ± 0.11 | 0.017 ± 0.004 | 0.368 ± 0.116 | 0.017 ± 0.001 |
| Type 2 diabetic | 1.08 ± 0.40 | 0.049 ± 0.033 | 0.942 ± 0.389 | 0.018 ± 0.007 |
| Moderate (40) | | | | |
| Lean | 19.13 ± 3.70* | 0.032 ± 0.006 | 0.105 ± 0.034* | 0.141 ± 0.039 |
| Obese | 4.97 ± 0.84* | 0.043 ± 0.006 | 0.463 ± 0.134* | 0.051 ± 0.007 |
| Type 2 diabetic | 2.42 ± 0.47* | 0.022 ± 0.004 | 0.389 ± 0.090* | 0.048 ± 0.013 |
| High (120) | | | | |
| Lean | 11.72 ± 0.78† | 0.017 ± 0.002 | 0.136 ± 0.074 | 0.265 ± 0.054† |
| Obese‡ | 15.28 ± 2.16† | 0.028 ± 0.006 | 0.139 ± 0.061† | 0.147 ± 0.045 |
| Type 2 diabetic | 11.32 ± 2.10† | 0.035 ± 0.010 | 0.350 ± 0.133 | 0.208 ± 0.087† |

Data are means ± SE. * $P < 0.05$, analysis of variance between groups (lean, obese, type 2 diabetic) within insulin dose; † $P < 0.05$, analysis of variance for significant change between insulin doses within group (lean, obese, type 2 diabetic); ‡one subject failed PET scan.

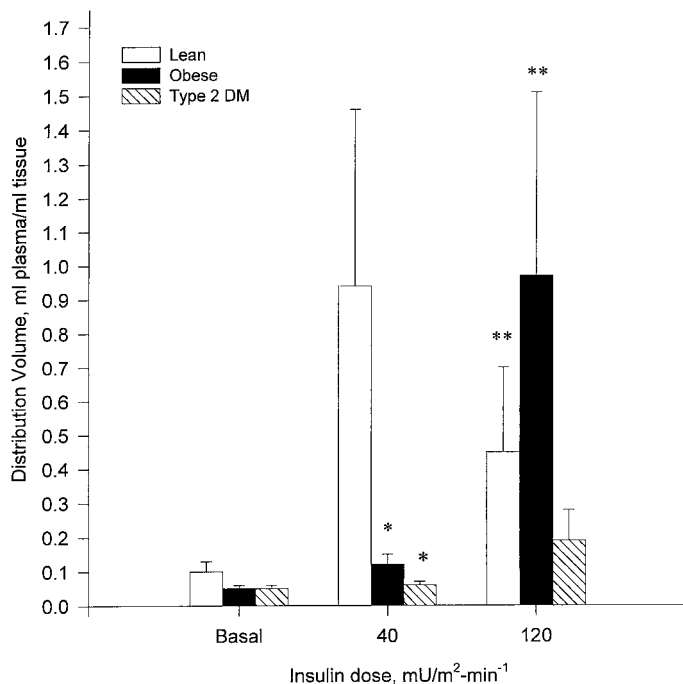


FIG. 4. Effect of insulin on the distribution volume (DV_{CE}) of [¹⁸F]FDG in lean (□), obese (■), and type 2 diabetic (▨) subjects. *The DV_{CE} was reduced at the moderate (40 mU/m² per min) insulin dose for obese and type 2 diabetic subjects when compared with lean subjects (*P* < 0.05). **The DV_{CE} was increased compared with the basal state at the high (120 mU/m² per min) insulin dose for the lean and obese subjects (*P* < 0.05).

seven- to tenfold greater in lean compared with the other two groups and did not differ in obese compared with type 2 diabetic subjects. Moreover, although the DV_{CE} and PF values were substantially increased compared with basal values in lean volunteers, in the obese and type 2 diabetic groups, these parameters of glucose transport and phosphorylation were only marginally and nonsignificantly increased compared with basal conditions.

High insulin infusion. During high rates of insulin infusion, group differences were far less evident. There was not a significant group difference in rates of [¹⁸F]FDG clearance (Table 3), PF (Fig. 5), or the rate constants of *k*₁ or *k*₃ (Table 3). The group differences noted for *k*₂ at moderate insulin were no longer significant. Within lean volunteers, there was relatively little difference in the rate constants in comparing results at moderate versus high ranges of insulin infusion. However, for the obese subjects, values for *K* and *k*₃ (Table 3), DV_{CE} (Fig. 4), and PF (Fig. 5) were strongly increased at the high versus the moderate rate of insulin infusion, and *k*₂ was significantly decreased compared with basal. In the type 2 diabetic subjects, the high rate of insulin infusion also resulted in stimulation of *K* and *k*₃ (Table 3) and PF (Fig. 5), though values for the rate constant *k*₂ remained elevated and DV_{CE} (Fig. 4) remained suppressed.

Relation of rate constants to LGU. Regression analysis was used to assess the relation of rate constants derived from dynamic PET imaging to glucose uptake determined simultaneously with leg-balance techniques. The correlation coefficients are shown in Table 4. LGU was significantly and positively correlated with overall FDG uptake (*r* = 0.81, *P* < 0.001). The relationship between LGU and *k*₁ did not reach statistical significance (*r* = 0.16, *P* > 0.10),

TABLE 4

Correlations between rate constants for [¹⁸F]FDG transport and phosphorylation, determined by dynamic PET, and assessments from leg balance studies across all groups and all insulin levels

| | Glucose fractional | | |
|--------------------------|--------------------|------------|----------------|
| | LGU | extraction | Leg blood flow |
| <i>K</i> | 0.81‡ | 0.82‡ | 0.44‡ |
| <i>k</i> ₁ | 0.16 | 0.05 | 0.16 |
| <i>k</i> ₂ | -0.38* | -0.48‡ | -0.12 |
| <i>k</i> ₃ | 0.53‡ | 0.58‡ | 0.28 |
| Distribution volume | 0.64‡ | 0.51‡ | 0.34* |
| Phosphorylation fraction | 0.76‡ | 0.87‡ | 0.36* |

**P* < 0.05, †*P* < 0.01, ‡*P* < 0.001.

whereas there was significant negative relation to *k*₂ (*r* = -0.38, *P* < 0.05), the rate constant for outward transport of [¹⁸F]FDG from skeletal muscle and positive correlation with DV_{CE} (*r* = 0.64, *P* < 0.001, Fig. 6A), the parameter of glucose transport. With respect to the kinetics of glucose phosphorylation, LGU was significantly correlated with *k*₃ (*r* = 0.53, *P* < 0.01) and the PF (*r* = 0.76, *P* < 0.001, Fig. 6B). Glucose fractional extraction, measured by arteriovenous leg balance, is a physiological parameter of the extent to which plasma glucose is trapped by skeletal muscle. This measure was strongly correlated with PF (*r* = 0.87, *P* < 0.001), which in turn represents a PET-derived index of glucose trapping. Glucose fractional extraction across the leg was also significantly related to several additional PET-derived rate constants. The correlations between leg blood flow and PET-derived rate constants were of lesser magnitude (Table 4).

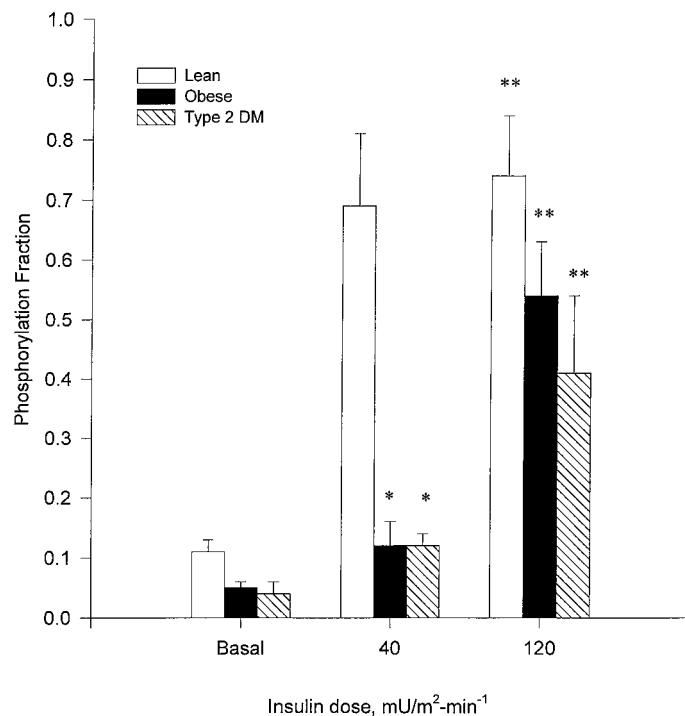


FIG. 5. Effect of insulin on the PF of [¹⁸F]FDG in lean (□), obese (■), and type 2 diabetic (▨) subjects. *The PF was reduced at the moderate (40 mU/m² per min) insulin dose for obese and type 2 diabetic subjects when compared with lean subjects (*P* < 0.05). **The PF was increased compared with the basal state at the high (120 mU/m² per min) insulin dose for the lean, obese, and type 2 diabetic subjects (*P* < 0.05).

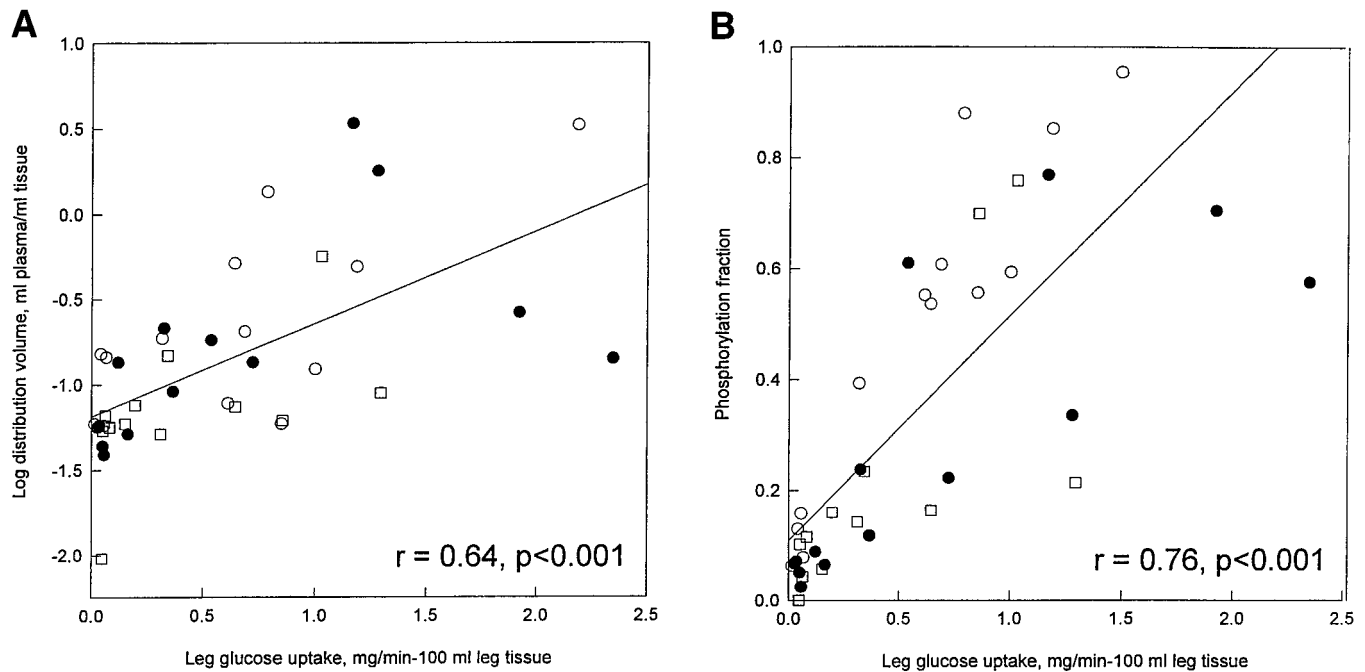


FIG. 6. Scatter plot of LGU, determined by leg-balance techniques, and distribution volume (A) and phosphorylation fraction (B), determined by dynamic PET imaging for lean (○), obese (●), and type 2 diabetic (□) subjects.

Stepwise multivariate regression analysis was used to further explore the relationship between PET-derived rate constants and LGU. Using LGU as the dependent variable and allowing the rate constants k_1 , k_2 , and k_3 to enter as the independent variables, the inclusion of k_2 and k_3 explained 46% ($P < 0.001$) of the variance in LGU with no additional significant contribution from k_1 . When the DV_{CE} and PF were used as the independent variables, the PF explained 63% ($P < 0.001$) of the variance in LGU with no additional ability to predict LGU contributed from the DV_{CE} . These models suggest that the efficiency with which [^{18}F]FDG is phosphorylated within skeletal muscle has a key role in determining the variance among insulin-sensitive and insulin-resistant subjects for skeletal muscle glucose metabolism.

TABLE 5
Fractional extraction of glucose, [^{18}F]FDG, [^3H]G, and the calculated LC

| Insulin dose (mU/min per m ²) | [^{18}F]FDG (%) | [^3H]G (%) | LC ([^{18}F]FDG/ [^3H]G) |
|--|----------------------------|-----------------------|---|
| Basal (0) | | | |
| Lean | 11.4 ± 4.4 | 10.5 ± 4.3 | 1.03 ± 0.28 |
| Obese | 14.6 ± 2.8 | 12.2 ± 2.7 | 1.34 ± 0.21 |
| Type 2 diabetic | 8.2 ± 1.4 | 6.9 ± 0.4 | 1.18 ± 0.13 |
| Moderate (40) | | | |
| Lean | 49.5 ± 10.0* | 37.1 ± 7.5* | 1.34 ± 0.04 |
| Obese | 11.8 ± 3.3* | 10.2 ± 3.0* | 1.23 ± 0.19 |
| Type 2 diabetic | 14.3 ± 2.8* | 11.3 ± 3.2* | 1.40 ± 0.21 |
| High (120) | | | |
| Lean | 46.5 ± 3.4† | 40.9 ± 4.1† | 1.15 ± 0.74 |
| Obese | 39.8 ± 3.7† | 30.8 ± 3.4† | 1.31 ± 0.49 |
| Type 2 diabetic | 37.5 ± 7.5† | 27.8 ± 6.6† | 1.41 ± 0.07 |

Data are means ± SE. * $P < 0.05$, analysis of variance between groups (lean, obese, type 2 diabetic) within insulin dose; † $P < 0.05$, analysis of variance for significant change between insulin doses within group (lean, obese, type 2 diabetic).

Determination of the LC. Values for the arteriovenous fractional extraction of [^{18}F]FDG and [^3H]G across the leg are shown in Table 5. The fractional extraction of [^{18}F]FDG and [^3H]G both increased in response to insulin dose ($P < 0.001$), and there was strong correlation between these parameters and the fractional extraction of glucose ($E_{[^{18}\text{F}]FDG}$: $r = 0.91$, $P < 0.001$; $E_{[{}^3\text{H}]G}$: $r = 0.90$, $P < 0.001$).

Values for the LC, calculated from the quotient of the fractional extraction for [^{18}F]FDG across the leg to that of [^3H]G, are also shown in Table 5. The arithmetic mean for the entire sample, across the three rates of insulin infusion, was 1.28 ± 0.08 . Values for the LC did not change significantly in relation to insulin infusion rate within or between groups. Shown in Fig. 7 is a regression plot of fractional extraction of [^{18}F]FDG and fractional extraction of [^3H]G. A highly significant correlation was observed ($r = 0.95$; $P < 0.001$), and the slope of this plot represents the value for the LC and is 1.22 ± 0.08 ($P < 0.001$) when forcing the y intercept through zero.

DISCUSSION

Classic dose-response studies of in vivo insulin action, performed using the glucose clamp method, demonstrate a rightward shift in obesity and type 2 diabetes (24). However, while these patterns indicate that the mechanisms of insulin resistance are malleable to insulin dose, it remains unclear which defects are mitigated by increased insulin concentration and whether some impairments remain fixed. Development of several in vivo methods for investigation of glucose transport and phosphorylation in skeletal muscle creates an opportunity to address the question of how proximal steps of glucose metabolism contribute to dose-response patterns of glucose metabolism (1–4, 6,7). The current study was undertaken with this purpose. Our laboratory, in a recent study using dynamic PET imaging of [^{18}F]FDG, found that in lean healthy individu-

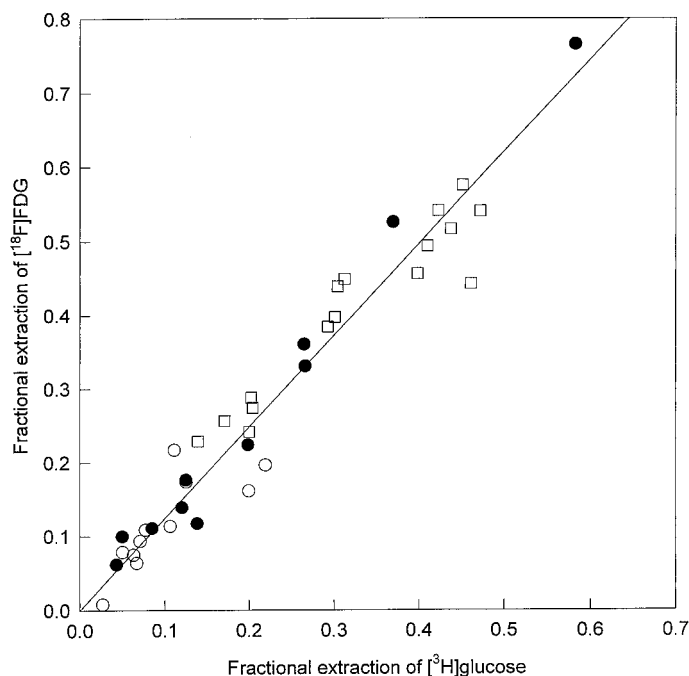


FIG. 7. Regression plot of fractional extraction of $[^{18}\text{F}]\text{FDG}$ and fractional extraction of $[^3\text{H}]\text{glucose}$ under basal (\circ), 40 mU/m^2 per min insulin (\bullet), and 120 mU/m^2 per min insulin (\square). The slope of this line is 1.22 ± 0.08 and represents the LC.

als, insulin not only modulates the kinetics of both glucose transport and glucose phosphorylation, but also modulates the interaction, or distribution of control, between these steps (7). In the current study, a rightward shift in the regulation of glucose transport and phosphorylation was found in type 2 diabetes and obesity. At a moderate level of insulin stimulation, there was insulin resistance of both glucose phosphorylation and glucose transport. The impairments were of similar severity in obesity and type 2 diabetes. However, these impairments were not fixed in severity. At a marked level of insulin stimulation, achieved with an infusion rate of 120 mU/m^2 per min, the impediment of glucose phosphorylation in skeletal muscle was substantially corrected in both type 2 diabetes and obesity. However, the parameters of glucose transport remained reduced in type 2 diabetes, whereas in obesity without type 2 diabetes, the impairment of glucose transport was alleviated. These dose-response findings suggest that in insulin resistance, as also found in insulin sensitivity, there is important dose-related insulin regulation of glucose transport and phosphorylation. The findings point not only to an impaired capacity for glucose transport, but also to an impairment in the efficiency of glucose phosphorylation in the pathogenesis of insulin resistance of skeletal muscle in obesity and type 2 diabetes. However, the contribution of impaired glucose phosphorylation appears to be chiefly evident at low to moderate levels of insulin stimulation. Thus, although this study confirms that glucose transport serves as a rate-limiting step for rates of glucose uptake during marked insulin concentrations, the data also provide fresh insight into the modulation of insulin resistance and the potential importance of the distribution of control between transport and phosphorylation in modulating insulin action.

Previously, during a study using dynamic PET imaging,

comparing fasting versus a single rate of insulin infusion, given at 40 mU/m^2 per min that achieved concentrations in the upper physiological range, individuals with type 2 diabetes were also found to have insulin resistance at both glucose transport and phosphorylation (6). Obese nondiabetic subjects in that study manifested an impairment of insulin-stimulated glucose transport that was of similar severity to that observed in type 2 diabetes, but they did not manifest a significant impairment of glucose phosphorylation. In the current study, the defect in glucose phosphorylation was evident in obesity as well as in type 2 diabetes. One reason for the difference may be that the subjects in the current study had more severe insulin resistance than the obese subjects of the prior investigation. Bonadonna et al. (2), using a forearm triple tracer method to study glucose transport and phosphorylation, also found impairment of both insulin-stimulated glucose transport and insulin-stimulated glucose phosphorylation in type 2 diabetes during moderate insulin stimulation. Therefore, like the data derived from dynamic PET imaging, the findings from the forearm triple tracer method indicate a major role for the two proximal steps of glucose metabolism in the pathophysiology of insulin resistance. However, to our knowledge, the studies using the forearm method have not examined dose-response modulation of these steps in relation to healthy volunteers or those with insulin resistance. Another method applied to assess the role of glucose transport and phosphorylation has been to ascertain muscle concentration of G-6-P using MRS (3,4). This approach is based on the postulate that an elevated level of G-6-P implicates a cause of insulin resistance beyond these initial steps, whereas a depressed level indicates an impediment at either or both glucose transport and phosphorylation. In lean healthy volunteers, insulin stimulates an increment in muscle concentration of G-6-P, whereas in keeping with a key role for these steps in the pathogenesis of skeletal muscle insulin resistance in type 2 diabetes, less increase of G-6-P is found (3,4).

One goal of the current study was to quantify the analog effect of $[^{18}\text{F}]\text{FDG}$ within skeletal muscles and to determine whether this is affected by either insulin concentration or insulin resistance. The analog effect was determined by comparing the arteriovenous uptake of $[^{18}\text{F}]\text{FDG}$ and $[^3\text{H}]\text{G}$ across the leg, each given as a bolus injection. The effect of insulin on the uptake of the analog and nonanalog glucose was very similar, as reflected by the plots of arteriovenous differences and by the strong overall correlation between fractional extractions of these two compounds. The respective ratio of uptakes, which is a determination of the LC for $[^{18}\text{F}]\text{FDG}$, was 1.2. This indicates a modest, preferential uptake of $[^{18}\text{F}]\text{FDG}$. Importantly, the LC was not different in obesity or type 2 diabetes, nor did it change significantly in response to insulin concentration. Thus, group differences with respect to rates of $[^{18}\text{F}]\text{FDG}$ uptake or the kinetics of transport and phosphorylation are not attributable to differences in analog effects of $[^{18}\text{F}]\text{FDG}$.

In the current study, the leg-balance (product of arteriovenous differences and blood flow) method was also used to determine rates of actual glucose uptake during steady-state conditions that prevailed during PET imaging. These measurements therefore provided simultaneous and inde-

pendent measures of glucose metabolism by the same tissue imaged using PET. Overall, across groups and insulin doses, there was strong correlation between rates of glucose uptake across the leg and rates of [^{18}F]FDG uptake into skeletal muscle. With regard to the respective contributions of glucose transport and phosphorylation in relation to LGU, both parameters had significant correlation. There was very strong correlation ($r = 0.87$) between the fractional extraction of glucose, which measures the extent of glucose trapping, and the kinetic parameter of glucose phosphorylation derived from modeling of dynamic PET imaging, which also reflects the efficiency of glucose trapped within muscle.

In the present data, the findings of a reduced value for transport parameter DV_{CE} are strong and are clear evidence that impaired glucose transport contributes to insulin resistance during both moderate and marked insulin stimulation. The current findings also indicate that efficiency of insulin stimulation of glucose phosphorylation is an additional determinant of glucose metabolism by skeletal muscle, with the important qualification that the dose-response patterns suggest that this effect is most important at low to moderate levels of insulin stimulation. Arguably, these are the conditions that are most pertinent to daily living. These findings in regard to redistribution of control by glucose transport and phosphorylation in insulin resistance of obesity and type 2 diabetes are consistent with patterns of redistribution of control observed in lean healthy volunteers during dose-response insulin infusion studies (7). In lean subjects, at the three doses used in the current study and with an additional low rate of insulin infusion (20 mU/m² per min), a dose-dependent insulin stimulation of glucose phosphorylation was observed in a pattern indicative of a key role in controlling glucose uptake during relatively low levels of insulin stimulation (7). However, in those data, as in the current study in obesity and type 2 diabetes, marked insulin stimulation appears to achieve near-maximal stimulation of glucose phosphorylation, and this shifts the locus of control toward glucose transport. Therefore, insulin not only acts to modulate activity at proximal steps of glucose metabolism, but also appears to further modulate the distribution of control that these steps exert over rates of glucose utilization in both lean and insulin-resistant subjects.

The observed changes in DV_{CE} and PF in lean subjects and at higher insulin doses in obese and type 2 diabetic subjects were in part driven by significant changes in k_2 . Moreover, the lack of change in DV_{CE} and PF at moderate insulin in obesity and type 2 diabetes was based largely on a lack of suppression of k_2 . The DV_{CE} is a classic PET parameter (19), whereas use of the PF as a PET parameter has been reported (22) but not as widely used. As noted in RESEARCH DESIGN AND METHODS, k_2 can represent [^{18}F]FDG that enters the interstitial space but is not transported into the tissue and [^{18}F]FDG that is transported into the tissue but not phosphorylated. Therefore, one might question whether group differences in the PF reflect primarily transport rather than phosphorylation impairments. Limiting analyses to the k_3 values alone revealed an ~10-fold increase from basal to maximal insulin stimulation in lean, obese, and type 2 diabetic subjects, with a more blunted effect at moderate insulin. Moreover, k_3 was the rate con-

stant with the strongest association with LGU. Thus, although both DV_{CE} and PF values are affected by k_2 and it is plausible that even the PF parameter could contain influences of impaired transport, the observed effects on the k_3 parameter indicate an independent contribution of impaired glucose phosphorylation.

In a recent investigation, Cline et al. (5) used microdialysis and MRS to estimate muscle concentrations of free glucose and MRS to estimate muscle G-6-P in order to better determine the respective roles of glucose transport and phosphorylation in the pathogenesis of insulin resistance in type 2 diabetes. Intracellular concentration of free glucose was estimated as the difference between interstitial glucose, determined by microdialysis, and free glucose in tissue and interstitium, determined by MRS. In type 2 diabetes, at a moderate insulin concentration, muscle G-6-P in type 2 diabetes was reduced compared with levels in nondiabetic subjects, whereas muscle free glucose was twofold greater, though this difference was not significant. During marked insulin concentrations, muscle G-6-P increased in muscle of type 2 diabetic subjects, albeit not to the level found in nondiabetic subjects during moderate dose insulin infusion, whereas free glucose concentrations were reduced. The findings of Cline et al. (5) during marked insulin concentration were interpreted as consistent with a rate-limiting impediment at glucose transport. The findings of the current study, during marked insulin concentrations, are also consistent with this interpretation. Yet, it should also be considered that the patterns found in the study by Cline et al., in the transition from moderate to marked insulin concentrations, that of intracellular free glucose declining and G-6-P increasing in type 2 diabetes, are consistent with an effect of insulin to modulate the distribution of control between transport and phosphorylation, and with insulin resistance at both glucose transport and glucose phosphorylation during moderate levels of insulin stimulation. The current findings, though consistent with rate-limiting control by glucose transport at marked insulin stimulation, indicate that at moderate insulin concentrations, defects of both glucose transport and phosphorylation are evident in type 2 diabetes.

Assessment of the relative importance of glucose transport and phosphorylation in skeletal muscle glucose uptake is currently an area of active research (1–7). A major limitation of any study that attempts to address the relative roles of glucose transport and phosphorylation is that the intracellular concentration of free glucose is exceedingly small, necessitating modeling techniques (1,2,6,7) or other innovative approaches of assessment, such as MRS (3–5). Thus, in the absence of directly measurable concentrations of intracellular free glucose, optimal validation of any technique is difficult. Moreover, if intracellular free glucose could be reliably measured, modeling techniques would not necessarily be required. The quantification of glucose transport and phosphorylation in human skeletal muscle using [^{18}F]FDG PET has shown that a three-compartment model similar to the one used in this report can be used to characterize the first two steps of glucose metabolism in skeletal muscle (25).

Modeling techniques have the advantage of being able to make the maximum use of complex experimental data from biological systems to determine fractional transfer-

rate constants. However, as is often the case, modeling does not necessarily provide definitive answers to the questions raised but rather emphasizes the perhaps previously unrecognized importance of component parts of the system, thus highlighting untested assumptions and revealing the need for improved experimental design (27). One assumption of modeling techniques is that the material in individual pools is uniformly distributed. With the potential for an arterial to venous gradient of [^{18}F]FDG, this assumption of uniform distribution of material may not be appropriate and result in interstitial concentrations of [^{18}F]FDG that differ from arterial concentrations of [^{18}F]FDG. To test this hypothesis, modeling was repeated using varying weighting for the arterial and venous data as an input function. The input functions we chose to examine to address this question ranged from 100% arterial to 0% venous, 75% arterial to 25% venous, 50% arterial to 50% venous, and 25% arterial to 75% venous. This reexamination of input function, using the various weighted arterial/venous input functions, did not change the fundamental group differences reported. A similar issue occurs with the intracellular distribution of hexokinase, which has been proposed by some authors to be nonuniform throughout the cell (27), which may result in nonuniform distribution of [^{18}F]FDG-6-P. The potential effects of this nonuniform distribution cannot be determined from the current data. Further optimization of the current study could be obtained with measures of flow rates. Blood flow was measured in this study using plethysmography, and rates did not differ between subjects. Incorporation of better measures of flow may be indicated to further elucidate the rate-limiting steps.

Another issue in the interpretation of these data is that [^{18}F]FDG is an analog of glucose. Prior *in vitro* studies have shown that the affinity of [^{18}F]FDG for the glucose transporter when compared with glucose is similar in rat heart (28) and up to 70% higher in rat brain (29). In both the rat heart and brain, the phosphorylation rate constant of [^{18}F]FDG is 60% that of glucose (28,29). If [^{18}F]FDG is preferentially transported in comparison to glucose and glucose is preferentially phosphorylated in comparison to [^{18}F]FDG, this would suggest that use of [^{18}F]FDG would theoretically underestimate the role of transport and overestimate the role of phosphorylation found in our results (30). However, the affinity of [^{18}F]FDG relative to glucose for glucose transporters and hexokinase in humans is less clear and has not been well studied in human skeletal muscle or insulin-resistant states. The LC value of 1.2, which is dependent on relative rates of both transport and phosphorylation of [^{18}F]FDG, suggests a slight overall preferential uptake of [^{18}F]FDG over glucose (10,11,31), and this ratio was not altered under varying degrees of insulin stimulation or insulin resistance. Thus, although the absolute rates of glucose transport and phosphorylation may not be predicted with 100% accuracy, we feel that group comparisons are valid.

In summary, physiological modeling of the kinetics of data on insulin-stimulated dynamic PET imaging of [^{18}F]FDG uptake into skeletal muscle suggests that across the range of insulin stimulation there is a distribution of control between the steps of glucose transport and phosphorylation. The efficiency of glucose phosphorylation has

an important influence over glucose metabolism that is particularly evident at low to moderate rates of insulin stimulation. In the setting of insulin resistance of obesity and obesity complicated by type 2 diabetes, there is impaired efficiency of glucose phosphorylation and this is especially severe within the range of insulin stimulation occurring in daily living. These findings reemphasize the importance of proximal steps of glucose metabolism, and perhaps especially of glucose phosphorylation, as a determinant of insulin resistance.

ACKNOWLEDGMENTS

These studies were supported by the University of Pittsburgh General Clinical Research Center (#5MO1RR00056), a Veterans Affairs Merit Award (to D.E.K.), and a National Institutes of Health Research Training in Diabetes and Endocrinology grant (#2T32DK07052-22 [to K.V.W.]).

We are grateful to our research volunteers and for the support of the nurses and research technicians at the General Clinical Research Center and the Positron Emission Tomography Center of the University of Pittsburgh. We would also like to acknowledge the technical expertise of Sue Andreko and Janice Beattie, the assistance of Brian Lopresti and Rob Sembrat with the determination of plasma arterial and venous curves, and the assistance of Cristy Matan with the analysis of the PET data.

REFERENCES

1. Saccomani MP, Bonadonna RC, Bier DM, DeFronzo RA, Cobelli C: A model to measure insulin effects on glucose transport and phosphorylation in muscle: a three-tracer study. *Am J Physiol* 270:E170-E185, 1996
2. Bonadonna RC, Del Prato S, Bonora E, Saccomani MP, Gulli G, Natali A, Frascerra S, Pecori N, Ferrannini E, Bier D, Cobelli C, DeFronzo RA: Roles of glucose transport and glucose phosphorylation in muscle insulin resistance of NIDDM. *Diabetes* 45:915-925, 1996
3. Rothman DL, Shulman RG, Shulman GI: ^{31}P nuclear magnetic resonance measurements of muscle glucose-6-phosphate: evidence for reduced insulin-dependent muscle glucose transport or phosphorylation activity in non-insulin-dependent diabetes mellitus. *J Clin Invest* 89:1069-1075, 1992
4. Rothman DL, Magnusson I, Cline G, Gerard D, Kahn CR, Shulman RG, Shulman GI: Decreased muscle glucose transport/phosphorylation is an early defect in the pathogenesis of non-insulin-dependent diabetes mellitus. *Proc Natl Acad Sci U S A* 92:983-987, 1995
5. Cline GW, Petersen KF, Krssak M, Shen J, Hundal RS, Trajanoski Z, Inzucchi S, Dresner A, Rothman DL, Shulman GI: Impaired glucose transport as a cause of decreased insulin-stimulated muscle glycogen synthesis in type 2 diabetes. *N Engl J Med* 341:240-246, 1999
6. Kelley DE, Mintun MA, Watkins SC, Simoneau JA, Jadali F, Fredrickson A, Beattie J, Theriault R: The effect of non-insulin-dependent diabetes mellitus and obesity on glucose transport and phosphorylation in skeletal muscle. *J Clin Invest* 97:2705-2713, 1996
7. Kelley DE, Williams KV, Price JC: Insulin regulation of glucose transport and phosphorylation in skeletal muscle assessed by positron emission tomography. *Am J Physiol* 40:E361-E369, 1999
8. Sheperd PR, Kahn BB: Glucose transporters and insulin action: implications for insulin resistance and diabetes mellitus. *N Engl J Med* 341:248-257, 1999
9. Wilson JE: Hexokinases. *Rev Physiol Biochem Pharmacol* 126:65-198, 1995
10. Kelley DE, Williams KV, Price JC, Goodpaster BH: Determination of the lumped constant for [^{18}F]FDG in human skeletal muscle. *J Nucl Med* 40:1798-1804, 1999
11. Peltoniemi P, Lonnroth P, Oikonen V, Tolvanen T, Gronroos T, Strindberg L, Takala T, Ruotsalainen U, Knuuti J, Nuutila P: The lumped constant for [^{18}F]fluoro-deoxy-glucose in human skeletal muscle, measured simultaneously with PET and microdialysis (Abstract). *Diabetes* 48 (Suppl. 1):A296, 1999
12. Hamacher K, Coenen HH, Stocklin G: Efficient stereospecific synthesis of non-carrier-added 2-[^{18}F]fluoro-2-deoxy-D-glucose using aminopolyether supported nucleophilic substitution. *J Nucl Med* 27:235-238, 1986

13. Barnes D, Egan G, O'Keefe G, Abbott D: Characterization of dynamic 3-D PET imaging for functional brain mapping. *IEEE Trans Med Imaging* 16:261–269, 1997
14. Bailey DL, Young H, Bloomfield PM, Meilke SR, Glass D, Myers MJ, Spinks TJ, Watson CC, Luk P, Peters M, Jones T: ECAT ART: a continuously rotating PET camera. performance characteristics, initial clinical studies, and installation considerations in a nuclear medicine department. *Eur J Nucl Med* 24:6–15, 1997
15. Watson CC, Newport D, Casey ME: A single scatter simulation technique for scatter correction in 3-D PET. *Proceedings of the 1995 International Meeting on Fully Three-Dimensional Image Reconstruction in Radiology and Nuclear Medicine*, 1995, p. 215–219
16. Ollinger JM: Model-based scatter correction for fully 3-D PET. *Phys Med Biol* 41:153–176, 1996
17. Colberg SR, Simoneau JA, Thaete FL, Kelley DE: Skeletal muscle utilization of free fatty acids in women with visceral obesity. *J Clin Invest* 95:1846–1853, 1993
18. Sokoloff L, Reivich M, Kennedy C, Des Rosiers MH, Patlak CS, Pettigrew KD, Sakurada O, Shinohara M: The [¹⁴C]deoxyglucose method for the measurement of local cerebral glucose utilization: theory, procedure, and normal values in the conscious and anesthetized albino rat. *J Neurochem* 28:897–916, 1977
19. Huang S, Phelps ME: Principles of tracer kinetic modeling in positron emission tomography and autoradiography. In *Positron Emission Tomography and Autoradiography: Principles and Applications for the Brain and Heart*. Phelps ME, Mazziotta JC, Schelbert HR, Eds. New York, Raven Press, 1986, p. 287–346
20. Huang SC, Phelps ME, Hoffman EJ, Sideris K, Selin CJ, Kuhl DE: Noninvasive determination of local cerebral metabolic rate of glucose in man. *Am J Physiol* 238:E69–E82, 1980
21. Dhawan V, Moeller JR, Strother SC, Evans AC, Rottenberg DA: Effect of selecting a fixed dephosphorylation rate on the estimation of rate constants and rCMRglu from dynamic [¹⁸F]fluorodeoxyglucose/PET data. *J Nucl Med* 30:1483–1488, 1989
22. Furler SM, Jenkins AB, Storlien LH, Kraegen EW: In vivo location of the rate-limiting step of hexose uptake in muscle and brain tissue of rats. *Am J Physiol* 261 (3 Pt 1):E337–E347, 1991
23. Zierler K: Theory of the use of arteriovenous concentration differences for measuring metabolism in steady and non-steady states. *J Clin Invest* 40:2111–2125, 1961
24. Kolterman OG, Gray RS, Griffin J, Burstein P, Insel J, Scarlett JA, Olefsky JM: Receptor and postreceptor defects contribute to the insulin resistance in noninsulin-dependent diabetes mellitus. *J Clin Invest* 68:957–969, 1981
25. Reinhardt M, Markus B, Vosberg H, Herzog H, Hubinger A, Reinauer H, Muller-Gartner H: Quantification of glucose transport and phosphorylation in human skeletal muscle using FDG PET. *J Nucl Med* 40:977–985, 1999
26. Carson ER, Jones EA: Use of kinetic analysis and mathematical modeling in the study of metabolic pathways in vivo. *N Engl J Med* 300:1016–1027, 1979
27. Vogt C, Yki-Jarvinen H, Iozzo P, Pipek R, Pendergrass M, Koval J, Ardehali H, Printz R, Granner D, DeFronzo R, Mandarino L: Effects of insulin on subcellular localization of hexokinase II in human skeletal muscle in vivo. *J Clin Endocrinol Metab* 83:230–234, 1998
28. Huang SC, Williams BA, Barrio JR, Krivokapich J, Nissenson C, Hoffman EJ, Phelps ME: Measurement of glucose and 2-deoxy-2-[¹⁸F]fluoro-D-glucose transport and phosphorylation rates in myocardium using dual-tracer kinetic experiments. *FEBS Lett* 216:128–132, 1987
29. Crane PD, Pardridge WM, Braun LD, Oldendorf WH: Kinetics of transport and phosphorylation of 2-fluoro-2-deoxy-D-glucose in rat brain. *J Neurochem* 40:160–167, 1983
30. Doest T, Han Q, Goodwin GW, Guthrie PH, Taegtmeier H: Insulin does not change the intracellular distribution of hexokinase in rat heart. *Am J Physiol* 275:E558–E567, 1998
31. Utriainen T, Lovisatti S, Makimattila S, Bertoldo A, Weintraub S, DeFronzo R, Cobelli C, Yki-Jarvinen H: Direct measurement of the lumped constant for 2-deoxy-[1-(¹⁴C)]glucose in vivo in human skeletal muscle. *Am J Physiol Endocrinol Metab* 279:E228–E233, 2000